Optimising Building-to-Building and Building-for-Grid Services under Uncertainty: A Robust Rolling Horizon Approach

Saman Nikkhah, *Graduate Student Member, IEEE*, Adib Allahham, Mohammad Royapoor, Janusz W. Bialek, *Fellow, IEEE* , and Damian Giaouris

***Abstract*— Energy systems are undergoing radical changes that have resulted in buildings being regarded as proactive players with the potential to contribute positively to energy networks. This study investigates the role of active buildings (ABs) as prosumers in energy systems by introducing a building-to-building (B2B) strategy for energy exchange between residential units, as well as a building-for-grid (B4G) model by exploiting the demand flexibility of residential microgrids (RMGs). The mid-market rate mechanism is adopted to produce local market price signals at RMG level. A robust rolling horizon controller is developed for real-time energy management of a community of ABs. This control philosophy can improve the robustness of the RMG in face of real-time weather and energy price prediction errors. The proposed method is a multi-level optimisation which pursues multiple goals while making a trade-off between operational cost and occupant comfort. Finally, the repercussions of COVID-19 induced power consumption resulting from changing lifestyle and building occupancy profile is analysed by the proposed method as a case study. The results show that the proposed B2B and B4G strategy can reduce energy bills by 18.45%, while notable robust real-time control and computational efficiencies are achieved when benchmarked against conventional methods.**

***Index Terms*—Active building (AB), robust rolling horizon (RRH), building-to-building (B2B), building-for-Grid (B4G).**

NOMENCLATURE

Indices

i	Index of tasks
j	Index of buildings
o	Operation period of building appliances
t	Index of time periods

Sets

ψ_i	Set of tasks
ψ_j	Set of buildings
ψ_n	Set of linearisation intervals
ψ_t	Set of time periods
$\psi_{t_j}^{oc}$	Set of occupied periods of building j

Parameters

$\hat{P}_{j,t}^{PV_F}$	Predicted photovoltaic unit output [kW]
$\hat{T}_t^{out}$	Predicted outdoor temperature [°C]
$\hat{V}_t^N$	Predicted outdoor illuminance level [lux]
$T_{j,t}^{Set}$	Temperature set point [°C]
$V_{j,t}^{Set}$	Illumination set point [lux]
β	Tolerable value of robustness
Δt	Duration of time periods [hour]
$\eta_I^{u/m}$	Utilization/maintenance factor of lightening devices
$\hat{\lambda}_t^{I/E}$	Predicted electricity import/export price $[£/kWh]$
κ_j	Number of lightening devices in building j
λ_t^G	Gas energy price $[£/kWh]$
A_j	Illuminated space in building j $[m^2]$
B	Total number of buildings
D_j^{th}	Thermal capacitance of building j [°C/kWh]
$E_{u/l}^{ESS}$	Maximum/minimum state of charge of energy storage [kWh]
f_j	Source flux value of building j
P_R^{CHP}	Rated power of combined heat and power [kW]
$P_{j,i,o}^{Ap}$	Power consumption of each task [kW]
P_u^G	Maximum power exchange rate with the main grid [kW]
$P_u^{ESS_{c/d}}$	Maximum charge/discharge rate of each building [kW]
R_j^{th}	Thermal reactance of building j [°C/kW]
T_j^{oc}	Total occupied periods of building j
$T_{j,t}^{B_{u/l}}$	Maximum/minimum temperature inside building j [°C]
$V_{j,t}^{B_{u/l}}$	Maximum/minimum Illuminance level [lux]
$\omega_{j,t}^{V/T}$	Visual/thermal weight factors

Variables

$(G/D)_t^{RMG}$	Total generation/demand capacity of RMG [kW]
$\alpha^{w/p}$	Weather related/market price robustness degree
$\chi_{j,i,t}^{Ap}$	Binary variable denoting the ON/OFF status of building appliances
$\chi_{j,t}^G$	Binary variable denoting the import/export power from main grid
$\chi_{j,t}^{ESS_{c/d}}$	Charging/discharging binary variables of energy storage
E_t^{ESS}	State of charge of energy storage [kWh]
$H_{j,t}^{HP/CHP}$	Output power of combined heat and power for heating purpose [kW]
$P_{j,t}^I$	Power consumption rate of each lighting device in building j [kW]
$P_{j,t}^{B2B}$	Active power of building j at time period t under B2B strategy [kW]
$P_{j,t}^{B4G}$	Active power of building j at time period t under B2B strategy [kW]
$P_{j,t}^{buy/sell}$	Buying/selling power inside RMG [kW]
$P_{j,t}^{ESS_{c/d}}$	Charge/discharge power of each building from/to energy storage [kW]
$P_{j,t}^{PV/CHP}$	Output power of photovoltaic/combined heat and

This work was made possible through funding from Newcastle University and Engineering and Physical Sciences Research Council grant EP/S016627/1: Active building Centre. (*Corresponding author: Saman Nikkhah.*)

Saman Nikkhah, Adib Allahham, Mohammad Royapoor, and Damian Giaouris are with the School of Engineering, Newcastle University, Newcastle upon Tyne, UK (e-mails: s.nikhah2@newcastle.ac.uk, adib.allahham@newcastle.ac.uk, mohammad.royapoor@newcastle.ac.uk, damian.giaouris @newcastle.ac.uk).

Janusz W. Bialek is with Newcastle University, UK (e-mail: Janusz.bialek@ncl.ac.uk) and with Skolkovo Institute of Science and Technology (Skoltech), Russia (e-mails: j.bialek@skoltech.ru).

power [kW]
$P_{j,t}^{G_{I/E}}$ Imported/exported power from/to main grid [kW]
$T_{j,t}^{B}$ Indoor temperature of building j [°C]
$V_{j,t}^{B}$ Illuminance level of building j [lux]
$V_{j,t}^{T}$ Total illuminance level of building j [lux]

I. Introduction

A. Motivation

BUILDING'S relationship to energy systems are evolving due to onsite generation, smart appliances and demand-side response. 36% of global energy consumption is attributed to building's embodied and operational energy use [1]. One way to reduce building's environmental impact is optimal scheduling and control of building loads that can enable them to become active agents within the wider energy system. Such active buildings (ABs) can also exchange energy and information locally to form a residential microgrid (RMG) [2]. These dynamic characteristics have become crystallised in the concept of smart local energy systems that include a broad range of soft (i.e. digital and cyber) and hard (i.e. distributed generation) infrastructure components, and additionally underline the concept of peer-to-peer energy trading [3] within a cluster of ABs. As well as cost and carbon saving, ABs seek to facilitate greater user choice, enable the possibility of energy transaction between ABs and maximising the use of distributed energy resources.

This requires a paradigm shift in the management of occupant comfort, maximising self-consumption and autonomy (in RMG), and maintaining virtual inertia and integrity (in the whole system). These requirements present two distinct opportunities for an RMG controller that supervises a community of ABs and their incorporated assets; first optimising the use of its communally-shared portfolio of energy resources, and second exploiting the possibility of energy exchange between buildings and/or with the utility grid. Following these goals can create a coordinated paradigm between ABs and energy networks, while facilitating the creation of community markets. These strategies supported by advanced telecommunication to enable real-time energy scheduling could be an efficient replacement for conventional load shedding [4]. To realise this, an RMG controller needs to overcome several challenges, namely real-time data processing of advanced metering infrastructure, catering for occupant preferences, and satisfying a set of techno-economic constraints. RMG controllers should also be computationally (i.e. processing power/speed) and economically viable for a residential application.

B. Literature Review

Energy management and control of ABs have been widely investigated in the literature, with representative studies concerned with optimising the operation of RMG assets [5]. Zhang *et. al* [6] has shown that optimal management of RMG elements can bring about 30% cost saving. These optimal energy scheduling approaches are guided by interactive energy market participation and real-time pricing [7], [8] that provide a signal on how smart appliances and distributed energy resources are managed in an RMG. Smart appliances are grouped based on interpretation [9], operational dependency [10], and controllability [11].

These advances in the energy management of ABs, changed their perspective in the energy networks, demonstrating how these units can play their part actively in the energy networks while maintaining their user preferences [12]. Authors in [13] considered each building as an agent that can play its part in energy optimisation of an unbalanced distribution network. In [14], optimising the scheduling of controllable appliances is considered as an important factor which can contribute to demand supply. Alwan *et. al* [15] investigated the effect of dwelling units on voltage profile of the grid. In Reference [15], the authors have shown that energy management strategies within a group of buildings can be effective in reducing the voltage fluctuation. Moreover, the demand-side management has been considered as an effective approach in decreasing the negative effect of reverse power flow caused by distributed generation.

These scheduling and control methods generally consider the optimisation of two main objectives: energy cost and occupant's comfort. The former is common among AB studies, while the latter is considered as a separate objective function, turning the problem into a multi-objective task [13], [14], or integrated into the main goal either using weighting factors [15] or cost-based coefficients [16]. The majority of the aforementioned studies however consider non-linear comfort models with an optimised mixed integer non-linear programming (MINLP), which require a powerful processor and increases the computation time. In this regard, mixed integer linear programming (MILP) models are preferred to MINLP as they can provide efficient application in controlling building appliances [17].

A controller within an RMG should be able to respond to the control signals from the main grid in real-time [18]. Several frameworks have been introduced for this purpose that draw benefits from the idea of look-ahead control strategies such as rolling horizon [19]. For instance, in [20], the controller updates the input results in a two stage optimisation so as to supply the real-time demand, while the storage facilities in the building compensate the mismatch between real-time and day-ahead processes. Authors in [21] introduced a rolling horizon based real-time optimisation method so as to minimise the operational cost, while the distribution system controller is coordinated with the building to respond to operational constraints of the grid. The point that should be considered in the rolling horizon based methods is that a current decision is made based on the predictions of future inputs, which is not always accurate. This creates the possibility of sudden changes by variations in occupants' behaviour, operational time of different assets, building thermophysical characteristics as well as building-related renewable generation. This, at wider scale, is known as demand uncertainty which has always been a substantial challenge for system operators.

In order to account for the impact of multiple sources of uncertainty, in addition to rolling horizon based real-time approach, several other methods have been explored. These include stochastic optimisation [22], [23], information gap decision theory [24], robust optimisation [25], and chance-constrained optimisation [11]. Stochastic methods [22], [23] illustrate the impact of uncertainty on operational cost, the difference between buying and selling electricity from/to the main grid [22], and the scheduling pattern of building appliances [23]. Stochastic methods, nevertheless, require sizeable amount of information about uncertain data streams that result in notable computational expense [26].

C. Research Gap

In summary, a gap has been observed in existing literature to examine:

I The possibility of energy exchange between buildings while also managing occupants' thermo-visual comfort and his/her expressed preferences for domestic tasks (in the form of a schedule).

II Deconstructing the demand-side response to its sources of sensitivity to alterations of comfort level and timing- ON/OFF status – or load adjustment of home appliances.

III Considering the effect of uncertainty on the model predictive control based rolling horizon methods, as suggested in [27], while improving the robustness of this method against uncertainty. The uncertainty can influence the energy exchange between buildings and overall comfort level. Furthermore, role of building occupants in improving robustness in face of uncertainty needs more exploration.

IV Achieving [I]-[III] through a computationally efficient control method that could be utilised in a residential sector and does not require investment for an expensive processor.

D. Contributions

Hence, this study attempts to address this gap by proposing a multi-level real-time energy management for a community of buildings [1] which can actively co-operate to achieve local and global goals. A rolling horizon based method is adopted to receive real-time weather and energy price data, while the robustness in each consecutive dispatch time interval is increased (referred to as RRH hereafter) using the notion of information gap decision theory. The proposed RMG controller exploits flexibility in AB loads (through interruptible loads and building inertia) and shared distributed energy resources to introduce building-to-building (B2B) and building-for-grid (B4G) strategies. The mid-market rate approach is adopted in the AB community level to create a local pricing market. The proposed model is multi-level and multi-objective. While the latter makes a trade-off between energy bill and occupants comfort, the former can guarantee the preference/benefits of ABs in the local energy market. The proposed architecture is an MILP model which can be solved by commercial solvers. The performance of the proposed controller is benchmarked against a conventional controller, and also tested under atypical operational characteristics such as COVID-19 related lockdown condition in 2020 which further highlighted the critical nature of modern power systems planning. The main contributions of this paper are:

- A multi-level MILP optimisation model is proposed for RMGs, with consideration for occupant comfort and appliance/task constraints. Compared to current MILP models, the proposed solution allows greater asset/building participation using a linear robust controller that does not require excessive processing power (as opposed to the MINLP predecessors). It also pursues multiple goals in achieving an optimal energy management.
- Introducing an RRH controller to maximise the robustness of real-time energy management systems against prediction uncertainties at a lower computational time (compared to conventional controllers) while accounting for partial knowledge of input parameters.

[1]In this study, building refers to a generic UK type family house

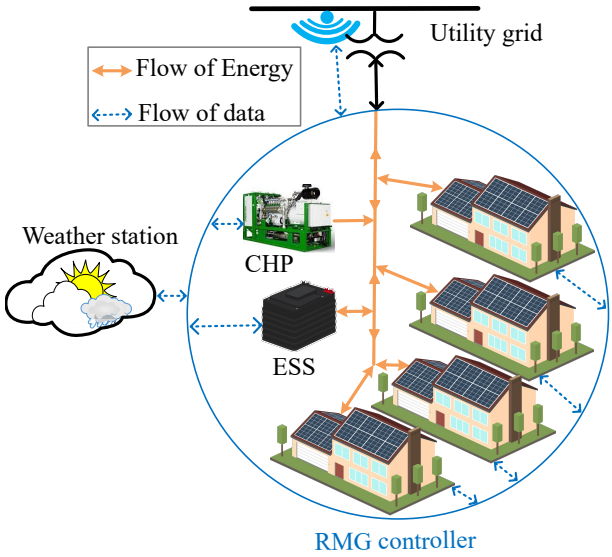

Fig. 1: The conceptual illustration of RMG.

- Proposing B2B and B4G strategies to oversee the peer-to-peer energy trading in RMG level while valuing the occupants comfort, and appliance settings under an uncertain environment. The former strategy facilitates the power exchange between dwellings using flexibility in in-site generation capacity, while the latter deconstructs the demand-side response to its sources of sensitivity to alterations of comfort level and timing- ON/OFF status – or load adjustment of home appliances.
- Taking into account the effect of multiple sources of uncertainty on the local energy markets, while exploring the role of building occupants in improving RMG robustness.

E. Article Structure

The remainder of this paper is organised as follows. Section II illustrates the concept of RMG. Section III outlines formulation of problem. Section IV explains different stages of the proposed multi-level control scheme. The framework description and simulation setup are introduced in Section V. Simulation results are discussed in Section VI and Section VII concludes the article.

II. Overview of Residential Microgrid Controller

A. The Residential Microgrid (RMG) Structure

A bidirectional transaction framework is required for successful data and energy exchange in an RMG. This concept is summarised in Fig. 1. Each AB is equipped with an individual photovoltaic unit, while combined heat and power and energy storage units are shared between the entire community given their high capital cost. The controller communicates internally with all ABs, the shared combined heat and power and energy storage and externally with a weather forecast platform (e.g. website queries) and the grid. The controller is assumed to access occupant preferences through digital media (i.e. mobile phone apps) to receive [I] day-ahead scheduled time for home tasks, [II] the preferred zone comfort thresholds, and [III] occupancy profile. This is augmented by real-time energy prices and weather-related data.

Based on this data platform, the controller performs a multi-level real-time optimisation of scheduled tasks within the RMG, and communicates subsequent control signals to each building, while the amount of energy that is required

from the upstream network is sent to the distribution grid controller. The optimal starting time of each task, cost and comfort level, the output of building level (photovoltaic unit) and community level (energy storage, and combined heat and power) assets, and the value of B2B/B4G transactive tasks is then communicated by the controller. Cloud computing is assumed to enable real-time communication and control signal processing, while observing privacy issues. Therefore:

- Real-time communication is assumed and a delay has not been considered.
- The RMG controller is in charge of the entire RMG asset-base and all AB asset data.
- RMG is connected to the main grid at point of integration.
- The energy sources within each building (e.g. photo-voltaic unit) are controlled by RMG controller.

B. Robust Rolling Horizon (RRH) Controller

The rolling horizon approach, which is based on the concept of model predictive control, can be used for real-time energy management of RMGs. This method uses real-time data for each discrete time interval to solve the optimisation over a nominal control horizon while also accounting for future time-slots. Therefore at time period t_1, the input data for upcoming intervals (i.e. $t_2 ... t_n$) are forecasted, so the optimised results are defined based on a predicted path. Forecast data uncertainty (especially for parameters prone to wide fluctuation) results in a simulation error (i.e. the difference between predicted and actual value). To reduce error, the conventional methods use smaller time intervals (i.e. reducing optimisation interval from 30min to 5min). However, this requires high computational time and power which may present difficulties when performing real-time controls. Additionally, smaller time intervals cannot solve the issue of future uncertainty. To address these issues, an information gap decision theory based technique has been proposed in this paper to increase the robustness of rolling horizon method. This method does not require excessive information on input parameters, and needs lower computational time compared to stochastic methods [26], making it suitable for dealing with input data with unknown behavioural patterns such as weather forecast. Generally,

Figure 2 attempts to illustrate this approach. In the conventional method (Fig. 2-a) [21] and at time instance t_1, the forecast error for a future instance of time (e.g. t_m) propagates into a simulation error. The proposed RRH method (Fig. 2-b) introduces a robustness degree for those input data that are more likely to change over operational horizon. By maximising the degree of robustness, the erroneous effect of the changeable forecasts on the control action is reduced. It should be noted that the optimal value of robustness is related to its tolerable value. The tolerable value of robustness is a parameter defined by the decision maker and increases the value of the objective function. This increase in cost is called cost of robustness. The bigger the tolerable value of robustness, the greater the system robustness. Therefore, in Fig. 2-b, the optimal value of dotted green line is related to the amount of increase in the objective function (i.e. from the solid green line to the dotted green line).

III. Problem Formulation

The proposed mathematical model describes optimal operation of multiple ABs, and shared energy sources, which form an RMG, while they can communicate with the utility grid, and locally together. In the following, the technical and operational

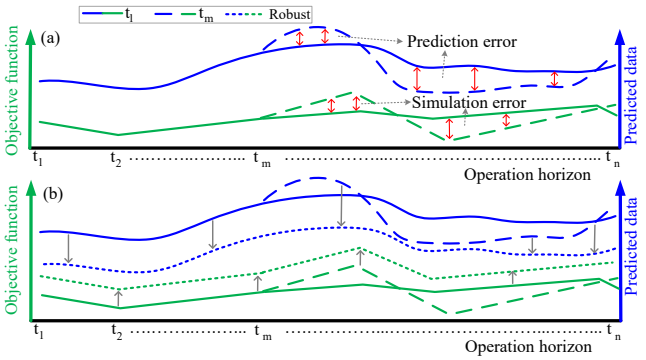

Fig. 2: Comparison of a) conventional rolling horizon, and b) the proposed RRH controllers.

constraints of RMG are introduced. Then, the AB flexibility strategies are discussed.

A. Objective Functions

In the proposed optimisation, the controller follows two conflicting objective functions, namely energy bill and occupants comfort index, defined as:

$$\min \left(\zeta = \Delta t \sum_{t \in \psi_t} \sum_{j \in \psi_j} \hat{\lambda}_t^{G_I} P_{j,t}^{G_I} - \hat{\lambda}_t^{G_E} P_{j,t}^{G_E} + \lambda_t^G P_{j,t}^{CHP} \right) \quad (1)$$

$$\max \left(\Xi = \frac{1}{B} \sum_{t \in \psi_{t_j}^{oc}} \sum_{j \in \psi_j} \frac{1}{T_j^{oc}} \left(\omega_{j,t}^V I_{j,t}^{V_{com}} + \omega_{j,t}^T I_{j,t}^{T_{com}} \right) \right) \quad (2)$$

where, Eq. (1) represents the energy bill, in which the first and second terms are cost and income of importing/exporting power from/to the main grid, respectively, while the third term is the cost of purchasing natural gas from the main grid for supplying the combined heat and power. The objective function given in (2) represents the comfort index of all ABs in the community (i.e.B) over the occupied period (i.e.T_j^{oc}) of each dwelling unit, which is obtained by multiplying the weighting factors $\omega_{j,t}^V$ and $\omega_{j,t}^T$ by virtual (i.e. $I_{j,t}^{V_{com}}$) and thermal (i.e. $I_{j,t}^{T_{com}}$) comfort indices respectively. While in predominant thermal comfort codes (i.e. BS EN ISO 7730, ASHRAE or Bedford) normally a 7 point approach is used to represent a 'too cold' to 'too hot' thermal spectrum, here for equation development this bidirectional band is translated into a single index of 0 to 1. Thermal neutrality (i.e. highest degree of comfort) is represented by 1 and degrees of departure from it (i.e. the space being too hot or too cold) moves the comfort index towards 0.

B. Operation of Different Tasks

Operational characteristics of AB appliances can be categorised into different groups, as outlined below.

Comfort-Providing Tasks: the consumption of these tasks is defined based on the preferred comfort level. Visual and thermal comfort-providing tasks are categorised into this group. Power consumption of these tasks is defined as:

$$V_{j,t}^B = \frac{\kappa_j P_{j,t}^I f_j \eta_I^u . \eta_I^m}{A_j} \quad (3)$$

$$T_{j,t+1}^B = T_{j,t}^B + \frac{\Delta t}{R_j^{th} D_j^{th}} \left(\hat{T}_t^{out} - T_{j,t}^B \right) + \frac{\Delta t}{D_j^{th}} H_{j,t}^{th} \quad (4)$$

where, in (3), $P^I_{j,t}$ is the amount of power consumed by lighting devices to provide visual comfort (i.e. $V^B_{j,t}$). Eq.(4) is widely referred to as building resistance and capacitance thermodynamic model [16], in which $H^{th}_{j,t}$ denotes the amount of power that is consumed for providing thermal comfort.

Fixed Power Consumption Tasks (i.e. ψ^F_i): set of tasks which operate in a specific period (i.e. ψ^{Ap}_{top}) with a fixed power consumption rate (e.g. cooker hob). Based on the preferred time window of these tasks, which is defined between their starting time (i.e.$\psi^{Ap}_{t_{st}}$) and ending time (i.e. $\psi^{Ap}_{t_{end}}$), their operation is described as:

$$\sum_{t=\psi^{Ap}_{t_{st}}}^{\psi^{Ap}_{t_{end}}-\psi^{Ap}_{top}} \chi^{Ap}_{j,i,t} = 1 \quad ,\forall i \in \psi^F_i \tag{5}$$

Variable Power Consumption Tasks (i.e. ψ^V_i): these tasks operate with a variable consumption rate, such as washing machine and dishwasher. Constraints (5) should be modified so as to describe the operation of these tasks, as follows:

$$\sum_{t=\psi^{Ap}_{t_{st}}}^{\psi^{Ap}_{t_{end}}} \chi^{Ap}_{j,i,t} P^{Ap}_{j,i,t} = \sum_{o=\psi^{Ap}_{top}} P^{Ap}_{j,i,o} \quad ,\forall i \in \psi^V_i \tag{6}$$

According to constraint (6), the ON/OFF status of each task (i.e. $\chi^{Ap}_{j,i,t}$) controls the required power at each period (i.e. $P^{Ap}_{j,i,t}$) so as to satisfy the variable power consumption at each operational period (i.e. $P^{Ap}_{j,i,o}$).

C. Comfort Constraints

The comfort indices are related to comfort related tasks as explained in (3)-(4). In addition to internal comfort providing technologies, outdoor illumination and temperature are considered as external factors which can affect the occupants comfort. These indices and their corresponding constraints are:

$$I^{V_{com}}_{j,t} = 1 - \left(\frac{V^T_{j,t} - V^{Set}_{j,t}}{V^{Set}_{j,t}}\right)^2 \tag{7}$$

$$V^T_{j,t} = V^B_{j,t} + \hat{V}^N_t \tag{8}$$

$$\begin{cases} V^{B_l}_j \le V^T_{j,t} \\ V^B_{j,t} \le V^{B_u}_j \end{cases} \quad ,\forall t \in \psi^{oc}_{t_j} \tag{9}$$

$$I^{T_{com}}_{j,t} = 1 - \left(\frac{T^B_{j,t} - T^{Set}_{j,t}}{T^{Set}_{j,t}}\right)^2 \tag{10}$$

$$T^{B_l}_j \le T^B_{j,t} \le T^{B_u}_j \tag{11}$$

where, (7) is the visual comfort index, while (8) shows the total illuminance level within each building, which is equal to the sum of natural illumination and that of lighting devices. Equation (9) limits the illuminance level. Besides, (10) represents the thermal comfort index, while (11) limits the buildings' indoor temperature. The quadratic term in (7) is linearised as follows:

$$\Omega^{V_+}_{j,t} + \Omega^{V_-}_{j,t} = \sum_{n=1}^{N} \theta^V_{j,t,n} \tag{12a}$$

$$0 \le \theta^V_{j,t,n} \le \theta^{V_u}_j \tag{12b}$$

$$V^T_{j,t} - V^{Set}_{j,t} = \Omega^{V_+}_{j,t} - \Omega^{V_-}_{j,t} \tag{12c}$$

$$\theta^{V_u}_j = \frac{V^{B_u}_j - V^{B_l}_j}{N} \tag{12d}$$

$$\gamma^V_{j,n} = (2n-1)\theta^{V_u}_j \tag{12e}$$

$$I^{V_{com}}_{j,t} = 1 - \left(\frac{\sum\limits_{n\in\psi_n} \gamma^V_{j,n}\theta^V_{j,t,n}}{\left(V^{Set}_{j,t}\right)^2}\right) \tag{12f}$$

where, N is the number of linearisation intervals. Based on the piecewise linearisation technique, the parabolic curve $(V^T_{j,t} - V^{Set}_{j,t})^2$ is approximated by variable $\theta^V_{j,t,n}$.

D. Energy Balance Constraints

In the designed RMG, heating and electricity energy demand of ABs is supplied by internal (e.g. combined heat and power and photovoltaic units) and external (e.g. electricity grid). The following energy balance constraints are introduced for the model.

$$\begin{aligned} &\sum_{i\in\psi_i}\left(\chi^{Ap}_{j,i,t-o}P^{Ap}_{j,i,o}\right) + P^I_{j,t} + P^{ESS_d}_{j,t} + P^{G_E}_{j,t} \\ &= P^{G_I}_{j,t} + P^{CHP}_{j,t} + P^{PV}_{j,t} + P^{ESS_c}_{j,t} + P^{B2B}_{j,t} \end{aligned} \tag{13}$$

$$H^{th}_{j,t} = H^{CHP}_{j,t} \tag{14}$$

where, (13) is the electric power balance, consisting of the consumption of different tasks and generation of various sources, while (14) represents the heating balance. The terms given in these equations are limited by their technical and operational constraints. The shared combined heat and power is the linking asset between heating and electricity energy.

E. RMG Asset Constraints

The central and individual energy providers of the RMG which are integrated to supply ABs load demand are limited by the following constraints.

$$\sum_{j\in\psi_j} P^{CHP}_{j,t} \le P^{CHP}_R \tag{15}$$

$$E^{ESS}_t - E^{ESS}_{t-1} = \Delta t\left(\sum_{j\in\psi_j}\eta^c_{ess}P^{ESS_d}_{j,t} - \sum_{j\in\psi_j}\left[\frac{P^{ESS_d}_{j,t}}{\eta^d_{ess}}\right]\right) \tag{16}$$

$$E^{ESS}_l \le E^{ESS}_t \le E^{ESS}_u \tag{17}$$

$$0 \le P^{ESS_c}_{j,t} \le \chi^{ESS_d}_{j,t} P^{ESS_d}_u \tag{18}$$

$$0 \le P^{ESS_d}_{j,t} \le \chi^{ESS_c}_{j,t} P^{ESS_c}_u \tag{19}$$

$$\chi^{ESS_c}_{j,t} + \chi^{ESS_d}_{j,t} \le 1 \tag{20}$$

$$\sum_{t\in\psi_t} P^{ESS_d}_{j,t} \le \sum_{t\in\psi_t} P^{ESS_c}_{j,t} \tag{21}$$

$$0 \le P^{PV}_{j,t} \le \hat{P}^{PV_F}_{j,t} \tag{22}$$

Constraint (15) limits the output power of combined heat and power based on its rated power, while $P^{CHP}_{j,t}$ could be

converted to $H_{j,t}^{CHP}$ by the the heat-to-power efficiency (i.e. η_{P2H}^{CHP}) of combined heat and power. Equations (16)-(21) describe the energy storage model, in which (16) denotes the total state of charge of energy storage, while it is limited by (17). In order to prevent net accumulation, the state of charge of battery at the end of the period (i.e. t_{end}) should be equal to its initial value at the beginning of the period (i.e. t_{st}). The charge and discharge of each building from the central storage is limited by (18) and (19) respectively. Note that the $P_u^{ESS_{c/d}}$ is also the maximum allowable charge/discharge of all ABs. Constraint (20) is a limiting logic based on the binary variables $\chi_{j,t}^{ESS_d}$ and $\chi_{j,t}^{ESS_c}$ which prevent simultaneous charge and discharge. Constraint (21) represents that the amount of discharged power for each AB is limited by the value of charged power. This means that AB j can utilise the power from energy storage if it has contributed to its charging before. Finally, constraint (22) represents the output power of rooftop photovoltaic units based on the predicted output.

F. Utility Grid

The RMG can receive and send electrical power from/to the utility grid. These limits are represented in the following constraints:

$$P_{j,t}^{G_I} \leq P_u^G \times \chi_{j,t}^G \tag{23}$$

$$P_{j,t}^{G_E} \leq P_u^G \times (1 - \chi_{j,t}^G) \tag{24}$$

where, binary variable $\chi_{j,t}^G$ prevents the simultaneous import and export from/to the main grid.

G. Active Building Flexibility Strategies

Active building strategies advance the role of prosumers in the energy network by introducing flexibility measures, while taking into account critical denominators such as users' comfort. These strategies can be divided to those which serve the AB community and those which provide services for the gird. The former is referred to as B2B strategy while the latter deconstructs the idea of demand flexibility into its source and is called B4G strategy.

Building-to-Building Strategy: this strategy is developed based on the idea of peer-to-peer energy trading [3]. According to this framework, buildings can participate in a local market based on their available generation capacity and demand flexibility. However, participating in peer-to-peer energy trading for an AB is subject to maintaining the techno-economic constraints and satisfying the occupant comfort. Furthermore, enrolling in B2B should bring about profit for each individual AB. This profit can be reflected in the energy bills. Finally, such a framework should not create security problems for the utility grid. The following equations represent the B2B strategy based on these criteria.

$$P_{j,t}^{B2B} = P_{j,t}^{buy} - P_{j,t}^{sell} \tag{25a}$$

$$0 \leq P_{j,t}^{buy} \leq P_{j,t}^{AB_D} - P_{j,t}^{AB_G} \tag{25b}$$

$$0 \leq P_{j,t}^{sell} \leq P_{j,t}^{AB_G} - P_{j,t}^{AB_D} \tag{25c}$$

$$0 \leq P_{j,t}^{buy} \leq (1 - \chi_{j,t}^{b2b}) \times M \tag{25d}$$

$$0 \leq P_{j,t}^{sell} \leq \chi_{j,t}^{b2b} \times M \tag{25e}$$

$$\sum_{j \in \psi_j} P_{j,t}^{B2B} = 0 \tag{25f}$$

The value of B2B for each AB and its role (i.e. buyer or seller) in the local market is defined by (25a). Each AB can specify its role as buyer (i.e. when $P_{j,t}^{B2B}$ takes its value from $P_{j,t}^{buy}$) or seller (i.e. when $P_{j,t}^{B2B}$ takes its value from $P_{j,t}^{sell}$) in the B2B framework by managing its generation capacity (i.e. $P_{j,t}^{AB_G}$) and demand (i.e. $P_{j,t}^{AB_D}$) as indicated by constraints (25b) and (25c) respectively. Constraints (25b) and (25c) also ensure that the energy exchange would happen based on the RMG internal capacities. Note that, the generation and demand of each individual AB are obtained in the energy balance equations. Based on constraints (25d) and (25e) each building can be a buyer or a seller in each time period. The variable $P_{j,t}^{B2B}$ is also added to the power balance equations in (13).

Building-for-Grid Strategy: for the B4G strategy, a positive variable is defined (i.e. $L_{j,i,t}^{flex}$) to tolerate the power consumption of the adjustable power consumption tasks, through multiplying it by the building appliances' power usage (i.e. $L_{j,i,t}^{flex} \times \chi_{j,i,t-o}^{Ap} \times P_{j,i,o}^{Ap}$). However, this will change the model to a non-linear one. Thus, the term $\chi_{j,i,t-o}^{Ap} P_{j,i,o}^{Ap}$ in (13) is replaced by $L_{j,i,t}^{flex} P_{j,i,o}^{Ap}$, while the following linear model is defined for B4G.

$$\chi_{j,i,t-o}^{Ap} \times L_l^{flex} \leq L_{j,i,t}^{flex} \leq \chi_{j,i,t-o}^{Ap} \tag{26}$$

$$P_{j,t}^{B4G} = \sum_{i \in \psi_i^v} P_{j,i,o}^{Ap} \times \left(\chi_{j,i,t-o}^{Ap} - L_{j,i,t}^{flex} \right) \tag{27}$$

where, constraint (26) introduces the upper and lower limits on the variable $L_{j,i,t}^{flex}$ based on the binary variable $\chi_{j,i,t-o}^{Ap}$ which has been defined in (5) for ON/OFF status of appliances. If a building appliance is on (i.e. $\chi_{j,i,t-o}^{Ap} = 1$), the upper value of $L_{j,i,t}^{flex}$ will be one, while the minimum value is defined by parameter L_l^{flex}. Constraint (27) represents the value of B4G which is non-zero if the flexibility variable would take a value less than one. The willingness of an AB to participate in this program depends on the market prices. Based on this strategy, ABs can respond to the price signal by turning appliances ON/OFF (i.e. $\chi_{j,i,t}^{Ap}$) or indeed where applicable adjust the value of flexibility (i.e. $L_{j,i,t}^{flex}$) to assist B4G services. To clarify, reducing the value of flexibility to an amount lower than one means the load of an appliance (or collection of appliances) can be adjusted. This means that the market price signal guides the controller to switch on appliances and adjust their consumption to bring about lower cost for ABs.

H. Pricing Mechanism

Participating in a local market can bring about several advantages for the prosumers, such as energy bill reduction, and improvement in energy system reliability [28]. In order to establish a local market and encourage ABs to participate in the B2B and B4G strategies, a suitable pricing mechanism is required. In this study, the mid-market rate method [29], a commonly used pricing mechanism, is adopted for establishing the energy prices within the RMG. The illustrative concept of this method is shown in Fig. 3. Based on this mechanism, the RMG local prices are defined as the average of import and export prices with the main grid (i.e. $\hat{\lambda}_{b2b,t}^{RMG} = (\hat{\lambda}_t^{G_I} + \hat{\lambda}_t^{G_E})/2$).

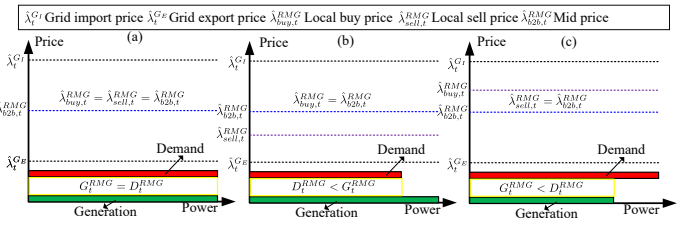

Fig. 3: Value of local market price under different demand-generation scenarios.

However, due to the fact that the RMG local generation (e.g. G_t^{RMG}) and demand (e.g. D_t^{RMG}) vary at each time-slot, three different scenarios are devised, as outlined below [29]:

I. RMG generation equals demand ($G_t^{RMG} = D_t^{RMG}$, as in Fig. 3-(a)): In this scenario, local buy (i.e. $\hat{\lambda}_{buy,t}^{RMG}$) and sell (i.e. $\hat{\lambda}_{sell,t}^{RMG}$) prices are equal to $\hat{\lambda}_{b2b,t}^{RMG}$. Local energy trading under this scenario happens with the average of grid import and export price. Therefore, buildings participating in the local market under this scenario can benefit from better buy and sell prices compared to those of the main grid.

II. RMG generation is higher than demand ($D_t^{RMG} < G_t^{RMG}$, as in Fig. 3-(b)): In this case, the local sell price is lower than average B2B price, while the excess generation can be sold to the main grid with the grid export price (i.e. $\hat{\lambda}_t^{G_E}$). Local buy price is equal to $\hat{\lambda}_{b2b,t}^{RMG}$ while local sell price is obtained by Eq. (28). Note that buildings with excess generation can sell their energy to the buyer buildings, whereas the amount of energy that could be sold to the main grid is proportionally allocated between all producers. This enables the fair distribution of price between all buildings in the community.

$$\hat{\lambda}_{sell,t}^{RMG} = \left(D_t^{RMG}\hat{\lambda}_{b2b,t}^{RMG} + (G_t^{RMG} - D_t^{RMG})\hat{\lambda}_t^{G_I}\right) \Big/ G_t^{RMG} \tag{28}$$

III. RMG generation is lower than demand ($G_t^{RMG} < D_t^{RMG}$, as in Fig. 3-(c)): The energy deficit is imported from the main grid with the grid price, while local sell price is equal to $\hat{\lambda}_{b2b,t}^{RMG}$ and local buy price is obtained by Eq. (29). The energy imported from the main grid is proportionally allocated to all consumers in the community.

$$\hat{\lambda}_{buy,t}^{RMG} = \left(G_t^{RMG}\hat{\lambda}_{b2b,t}^{RMG} + (D_t^{RMG} - G_t^{RMG})\hat{\lambda}_t^{G_E}\right) \Big/ D_t^{RMG} \tag{29}$$

Under this pricing framework, ABs can trade energy locally, while exchanging energy with the main grid based on the grid pricing contracts. As illustrated in Fig. 3, the local prices are defined between grid import and export prices. Therefore, participating in the local market brings profit to both buyers and sellers. Those who buy energy can benefit from lower price compared to that of grid import, while sellers can sell their excess generation with a price better than that of grid export price. In addition to the B2B strategy, the B4G method allows ABs to reduce their prices by utilising their demand flexibility. Accordingly, the energy bill of each AB is written as:

$$\zeta_j = \Delta t \sum_{t \in \psi_t} \left\{ \begin{array}{l} \hat{\lambda}_t^{G_I} P_{j,t}^{G_I} - \hat{\lambda}_t^{G_E} P_{j,t}^{G_E} + \lambda_t^{G} P_{j,t}^{CHP} \\ -\hat{\lambda}_t^{G_E} P_{j,t}^{B4G} \\ \hat{\lambda}_{buy,t}^{RMG} P_{j,t}^{buy} - \hat{\lambda}_{sell,t}^{RMG} P_{j,t}^{sell} \end{array} \right\} \tag{30}$$

IV. Proposed Multi-Level RMG Control Scheme

In order to accommodate the proposed mid-market rate pricing mechanism, B2B and B4G service provision models, the RMG controller has to consider three important factors. Firstly, it has to dispatch an ABs participation in B2B and B4G services only if that control action can provide added benefits (i.e. reduced energy bills). Secondly, participation in any local market for a building should honour occupant comfort constraints. Finally, the RMG controller should consider input parameter prediction errors when processing control signals for the community. To address these challenges, this study introduces a multi-level control framework as outlined in the following subsections.

A. Base-Case RMG Control (First Level)

An AB-specified market should present cost saving to the participants. In other words, energy bill of ABs after participating in the B2B and B4G should be lower than that without these strategies. Accordingly, the base-case level of the RMG control strategy minimises the energy bill in Eq. (1) without consideration for B2B and B4G constraints, as follows:

$$\min \left(\zeta^{l1} = \zeta\right) \tag{31a}$$

$$s.t: \quad (3) - (24) \tag{31b}$$

The value obtained for ζ^{l1} is considered as a constraints for other levels of optimisation. The value obtained for total RMG generation and load is also utilised to define the mid-market rate local prices. This allows the definition of local prices without consideration for an individual AB's benefit, bringing about a fair distribution of benefit among all dwellings.

B. Multi-Objective Optimisation (Second Level)

This level exploits B2B and B4G strategies to obtain the greatest energy bill saving. The willingness to minimise the cost, however, brings it into a conflict with the occupants comfort. In this regard, it is required to solve this level as a multi-objective optimisation. In this study, the $\epsilon-constrained$ method is adopted to solve the optimisation problem. This method does not require manual definition of weights and can deal with convex and non-convex methods as opposed to other approaches such as weighted sum technique [30]. These are important factors that should be considered, especially in automated control methods. In this method, one of the objective functions is transferred into the model constraints, while the other is optimised. The objective function that is considered as a constraint takes its limits from ϵ, which is derived from the maximum and minimum values of the objective function that is being considered as a constraint.

Noting that either objective function could be optimised, the energy bill is minimised in (32a) while the comfort level is defined as the model constraint in (32b). This process turns the model into a single-objective cost optimisation while the comfort level is constrained by ϵ. The value of ϵ is defined between maximum and minimum possible comfort level. The interval between the maximum and minimum value is divided into equal steps and the optimisation is solved for each value.

As aforementioned, energy bill with AB flexibility mechanisms should be lower; therefore, constraint (32c) is introduced

in this level. The other constraints of this optimisation are (3)-(27). This will enable the generation of all Pareto optimal solutions for a multi-objective problem.

$$OF = \min_{DV} \left(\sum_{j \in \psi_j} \zeta_j \right) \tag{32a}$$

$$s.t:$$

$$\Xi \geq \varepsilon \tag{32b}$$

$$\zeta_j \leq \zeta_j^{l1} \tag{32c}$$

$$(3) - (27) \tag{32d}$$

In (32), the operational cost is minimised while the value of ϵ is decreased from the maximum value of occupants comfort (obtained when Ξ is maximised solely) to its minimum value (obtained when ζ is minimised solely). Solving this optimisation problem draws a Pareto optimal set for both objective functions. Considering the fact that all Pareto optimal solution are acceptable, there is a need to select the best compromise solution. To do so, a fuzzy-based min-max method is adopted, in which the minimum value of each membership function is obtained, and the maximum value of the selected membership functions is chosen as the best compromise solution [30]. Note that constraint (32c) ensures that participating in the local market does not increase each individual AB's energy bills.

C. RRH Controller (Third Level)

The schematic illustration in Fig. 2 demonstrated that the deviation from predicted data can affect the simulation results. Since the proposed mid-market rate pricing mechanism is developed based on the generation capacity and AB demand, as well as the price signals, it is necessary to consider the effect of uncertainty on the B2B and B4G strategies.

The proposed method is a robust real-time energy management technique which is different from the stochastic optimisation. For more elaboration on this method, consider Fig. 4 [31]. As shown in this figure, stochastic methods require precise information on the uncertain input data. This information requires accurate knowledge about the probability density function of each uncertain parameter, which is a strenuous task in case of input data with unknown behavioural patterns. Furthermore, as illustrated in this figure, stochastic methods produce a large number of scenarios for each uncertain parameter, resulting in a dramatic increase in the computational time. On the other hand, the proposed method which is based on information gap decision theory technique, only requires an uncertainty set which does not need to be known. This method increases the immunity (i.e. robustness) of objective function in face of uncertainty in the input data. This means that the optimal value of objective function will remain immune if the input data vary within an unknown threshold.

This study utilises the envelope-bounded model of information gap decision theory to improve the robustness of RMG controller in face of uncertainty. This model is mathematically described as follows [32]:

$$U(\alpha, \widehat{\nu}) = \left\{ \nu : \left| \nu(t) - \widehat{\nu}(t) \right| \right\} \leq \alpha \left| \widehat{\nu}(t) \right|, \quad \alpha \geq 0 \tag{33}$$

where $\nu(t)$ is the value of uncertain variable which deviates around the predicted value (i.e. $\widehat{\nu}(t)$). The size of gap between

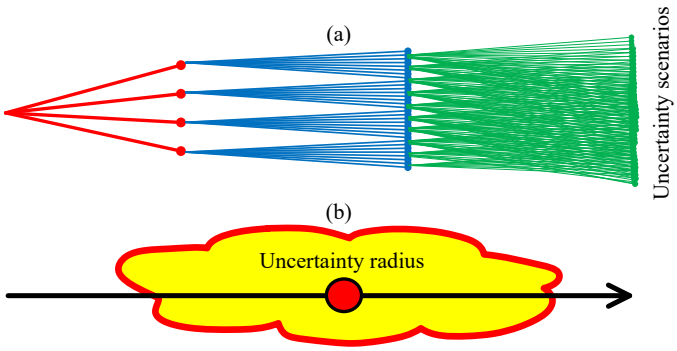

Fig. 4: The conceptual difference of a) stochastic optimisation, and b) information gap decision theory.

$\nu(t)$ and $\widehat{\nu}(t)$ is defined by α which is called uncertainty variable. Based on this model, the fractional deviation of predicted parameter from the uncertain value is limited by α. The bigger the value of α, the larger the horizon of deviation.

In the proposed model, the predicted values of outside temperature (i.e. $\hat{T}_t^{out}$), natural illuminance level (i.e. $\hat{V}_t^N$), and photovoltaic unit output (i.e. $\hat{P}_t^{PV_F}$) are considered as the weather-related uncertain data. While these parameters are weather-related, the first two data impose demand uncertainty while the third one reflects the generation uncertainty. The import/export electricity prices (i.e. $\hat{\lambda}_t^{I/E}$) are also considered as the market related components of uncertainty. It is worth mentioning that these sources of uncertainty can even affect the local market prices.

Since these parameters are more likely to experience variation over the control horizon, the proposed RRH controller improves the system robustness in face of market price deviation (i.e. α^p) and weather-related forecasted data uncertainty (i.e. α^w) over the control horizon by scheduling AB assets and benefiting from the participation of occupants. Note that these deviations will be obtained based on the control mechanism. To achieve this control philosophy, the RRH controller solves the following optimisation:

$$\max_{DV} \left\{ \alpha^t \left(\begin{array}{c} \min(\zeta) \times (1+\beta) \geq \zeta \\ \max(\Xi) \times (1-\beta) \leq \Xi \end{array} \right) \right\} \tag{34}$$

$$s.t:$$

$$\alpha^t = \omega \times \alpha^w + (1-\omega) \times \alpha^p \tag{35}$$

$$P_{j,t}^{PV} \leq (1-\alpha^w) \hat{P}_t^{PV_F} \tag{36}$$

$$V_t^N \leq (1-\alpha^w)\, \hat{V}_t^N \tag{37}$$

$$T_t^{out} \leq (1-\alpha^w) \hat{T}_t^{out} \tag{38}$$

$$\lambda_t^{I/E} \leq (1+\alpha^p) \hat{\lambda}_t^{I/E} \tag{39}$$

$$\zeta_j \leq \zeta_j^{l1} \tag{40}$$

$$(3) - (27) \tag{41}$$

In (34), the weighted sum method is utilised to obtain the maximum degree of robustness. The tolerable value of robustness degree which affects both objective functions is

specified by parameter β, which is defined in the interval [0,1]. Assuming that the weather-related data affect photovoltaic unit output, natural illuminance level, and outside temperature, the robustness degree is multiplied by these input parameters in (36)-(38) respectively. Also, the effects of market price robustness degree is obtained in (39). Robustness degrees are defined in the interval [0,1].

Knowing that the previous studies which have investigated a robust market price framework [24] introduced a non-linear model such as constraint (39) , this equation has been linearised in this study through replacing the term $\lambda_t^I P_{j,t}^{G_I}$ by the variables $P_{j,t}^{G_L^1}$ and $P_{j,t}^{G_L^2}$ as follows:

$$\lambda_t^I P_{j,t}^{G_I} = \left(P_{j,t}^{G_L^1}\right)^2 - \left(P_{j,t}^{G_L^2}\right)^2 \tag{42a}$$

$$P_{j,t}^{G_L^1} = \frac{1}{2}\left(\lambda_t^I + P_{j,t}^{G_I}\right) \tag{42b}$$

$$P_{j,t}^{G_L^2} = \frac{1}{2}\left(\lambda_t^I - P_{j,t}^{G_I}\right) \tag{42c}$$

where the non-linear terms in (42a) are linearised using the method described in (12). The same approach is adopted to linearising $\lambda_t^E P_{j,t}^{G_E}$ and $\lambda_t^E P_{j,t}^{B4G}$.

D. Decision Variables

The decision variables of proposed RRH control method consist of temperature and illuminance level in each building, radius of uncertainties, imported/exported power from/to the main grid, output value of distributed energy resources, value of B2B and B4G, and ON/OFF status of appliances. Note that the other variables such as local prices, consumption power for delivering comfort, comfort indices, and demand level of each building are dependent variables which are obtained through solving the proposed problem along with optimising the values of decision variables. The set of decision variables (i.e. DV in equations (34) and (32)) are defined as below:

$$DV = \left\{ \begin{array}{cc} T_{j,t}^B & \forall j \in \psi_j, t \in \psi_t \\ V_{j,t}^B & \forall j \in \psi_j, t \in \psi_t \\ \chi_{j,i,t}^{Ap} & \forall j \in \psi_j, t \in \psi_t, i \in \psi_i \\ P_{j,t}^{G_{I/E}} & \forall j \in \psi_j, t \in \psi_t \\ P_{j,t}^{PV/CHP} & \forall j \in \psi_j, t \in \psi_t \\ P_{j,t}^{ESS_{c/d}} & \forall j \in \psi_j, t \in \psi_t \\ P_{j,t}^{B2B} & \forall j \in \psi_j, t \in \psi_t \\ P_{j,t}^{B4G} & \forall j \in \psi_j, t \in \psi_t \\ \alpha^t & \end{array} \right\} \tag{43}$$

V. Framework Description and Simulation Setup

A. Framework Description

Fig. 5 illustrates the framework of the proposed RMG controller. The input data is transferred to the data receiver. Then, for the time period t, the model is solved in three levels, starting from the first level where energy bill is minimised without B2B and B4G strategies. The local prices are determined in this level, while the value of energy bill is considered as a constraint for outer levels. The second level takes into account two conflicting objective functions, while the process ends up with the RRH which improves the robustness of the model in the same time window. The linking variables between second and third levels are energy bill and occupants comfort.

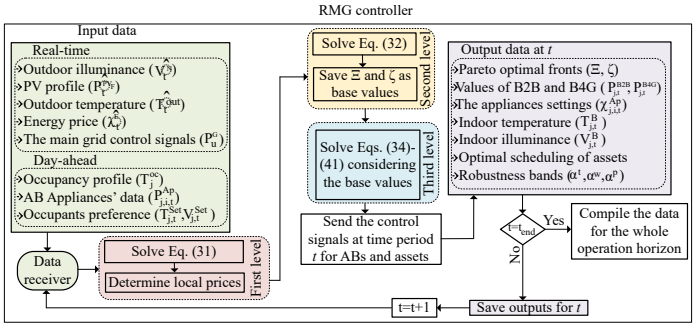

Fig. 5: Illustration architecture of the RMG controller.

TABLE I: building and task description.

building No.	Type	Included tasks No.	Task No.	Description
j_1	3	$i_1 - i_{10}$	i_1	Dishwasher
j_2	2	$i_1 - i_6, i_{10}$	i_2	Washing machine
j_3	2	$i_7 - i_{10}$	i_3	Spin dryer
j_4	1	$i_1 - i_4, i_6 - i_7, i_{10}$	i_4	Cooker hob
j_5	1	$i_4 - i_{10}$	i_5	Cooker oven
j_6	3	$i_1 - i_{10}$	i_6	Microwave
j_7	1	$i_1 - i_4, i_8 - i_{10}$	i_7	Laptop
j_8	1	$i_1 - i_4, i_6 - i_{10}$	i_8	Desktop
j_9	3	$i_1 - i_{10}$	i_9	Vacuum cleaner
j_{10}	2	$i_5 - i_7, i_9 - i_{10}$	i_{10}	Fridge

At the end of each time period, the controller sends the control signals to the ABs and different assets while re-compiles the process for the next time-slot. This process is continued until the end of operation horizon, when the results for the whole period is analysed.

B. Simulation Setup and Case Studies

The proposed problem is an MILP model which has been simulated in general algebraic modelling system (GAMS) [33] using CPLEX solver. The simulation is performed for 24 hours, using 30-minute time windows, starting from 8:00AM. 10 ABs are considered in the RMG. Buildings are categorised into three types as a function of their occupancy profile. Fig. 6 illustrates the occupancy profile and comfort weighting factor index for each AB under normal operating condition and then during a winter day. Buildings are categorised into three types as a function of their occupancy profile. The bold, white and pale colours represents occupied, unoccupied and sleeping periods respectively. The information on buildings and included tasks in each one is given in Table I. Other supporting data are available online at [34].

The effectiveness of the proposed model is evaluated by the following case studies:

Case I: The proposed model without B2B and B4G strategies. This case study solves the second and third levels of the optimisation without AB flexibility measures.

Case II: The proposed model with B2B and B4G strategies. This case study is solved for different scenarios.

Case III: The proposed model in an abnormal condition. Case II is solved under different occupancy profile where ABs are always occupied. This case attempts to represent an abnormal scenario such as COVID-19 pandemic lockdown which changed the occupancy profile of residential buildings.

VI. Results and Discussion

The results obtained for the proposed model are analysed and discussed in this section through comparison of various case studies. The computation efficiency of the model is also tested.

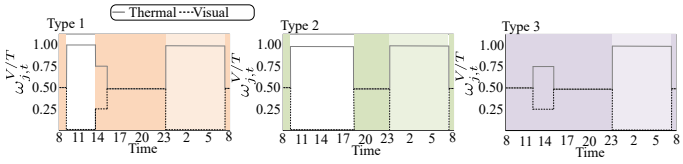

Fig. 6: Occupancy profile and comfort weights of different buildings types.

A. Pareto Optimal Solutions

In order to investigate the impact of different strategies over the operation horizon, the Pareto optimal fronts for cases I, II, and III reflecting different strategies are depicted in Fig. 7. In these solutions, the value of ϵ (i.e. comfort level) is decreased from its maximum value to its minimum value while the operational cost is minimised. For example, in Case I (shown in blue in Fig. 7), the value of comfort index is decreased from 0.992 to 0.965 in different levels while the operational cost is minimised for each level. Different solutions and case studies are highlighted and compared in this figure. The main observations are:

I. The Pareto optimal solutions: the cost-optimal solution decreased the comfort index to its minimum allowable level, while comfort-optimal solution seeks temperature and illuminance values that are closest to the set points, resulting in more expenditure for the community. This solution is compatible to the thermostats that are used in the majority of buildings. The compromise solution makes a trade-off between comfort and cost. This solution provides 16.46% lower energy bill compared to thermostat-controlled solution while keeping the comfort level close to set points (i.e. only 0.5% decrease compared to comfort-optimal solution). Therefore, this control framework could be a suitable alternative for the current thermostats in each building.

II. B2B and B4G strategies: it is evident from comparing the solutions for cases I and II that participating in the B2B and B4G strategies brought about better solutions (from both viewpoints of cost and comfort) for ABs. The compromise and robust solutions in Case II are about 18.45% and 18.46% lower than those of Case I. From the comfort index point of view, the robust solution in Case II is 1.1% higher than that of Case I, demonstrating the effect of the proposed AB flexibility strategies in improving occupants comfort with lower cost. This results imply that the flexibility measures can improve the socio-economic aspects of buildings, while demonstrating the importance of local energy markets. It is crucial to consider the fact that the problem is solved from the RMG's perspective, while the advantages for the main grid, no need for expansion planning for instance, are important factors that should be taken into account.

III. Robust solution: the robust solution imposed more cost, while the occupants' expectation is slightly decreased. For instance, in Case II, for a 10% robustness improvement (i.e. $\beta = 0.10$) the energy bill increases by 63 pence while the occupant comfort decreases 1.3%. This results demonstrates the role of building occupants in boosting the robustness of the proposed control strategy with a negligible cost.

IV. Cases II and III: Case III represents constantly occupied ABs and therefore has to deliver greater comfort at a higher cost. Note that increasing comfort levels in Case III also increases the overall energy system loads. Therefore, it is crucial to consider the fact that the pandemics (e.g. COVID-19) can change the consumption pattern of dwellings, which should be taken into account operation and planning of energy systems.

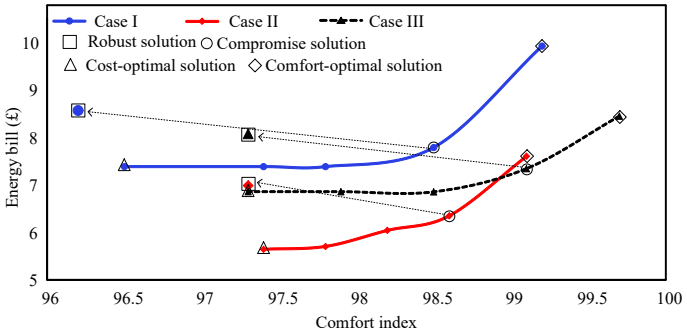

Fig. 7: Pareto optimal front for multiple optimisation solutions.

TABLE II: Root mean square error of Case III for each AB.

Building No.	j_1	j_2	j_3	j_4	j_5
Root mean square error (%)	2.42	15.41	15.44	6.75	6.75
Building No.	j_6	j_7	j_8	j_9	j_10
Root mean square error (%)	2.48	6.73	6.76	2.45	15.39

B. COVID-19 Effect

In order to analyse the impact of COVID-19 on the building load profile, the root mean square error of Case III is summarised in Table II. As can be seen in this table, the root mean square error of each building varies based on its type and occupancy profile before and after lockdown. This variation in the root mean square error value has been observed in the real-date analysed by Reference [35].

C. Building Flexibility Values

Figure 8 demonstrates Case II scenarios with the left picture outlining the power exchange between ABs in the B2B strategy and the right picture outlining the flexibility service provided by B4G strategy. As an illustration, consumption patterns of buildings j_1 (type three building), and j_{10} (type two building) are separately illustrated on the outer edges of the figure. In the B2B strategy, type three buildings (i.e. occupied the whole day) mostly played the role of the receiver, as opposed to type two buildings (i.e. unoccupied during office hours) which can provide other ABs with their available capacity. Another decisive factor in B2B strategy is the starting time and operation window of buildings appliances, such that the buildings that need to start their tasks at hours with high rates of market price received more energy, compared to other buildings in the same category. For instance, building j_1 received more energy than j_6. In B4G strategy, type three buildings (e.g. j_1) are more active as they are equipped with more adjustable power consuming appliances. On the other hand, type two buildings (e.g. j_{10}) did not participate actively since they do not offer a full range of adjustable appliances. The lower the number of tasks, the less an AB can contribute proactively to the grid in B4G strategy. Therefore, it can be concluded that B2B strategy creates flexibility based on generation capacity and occupancy

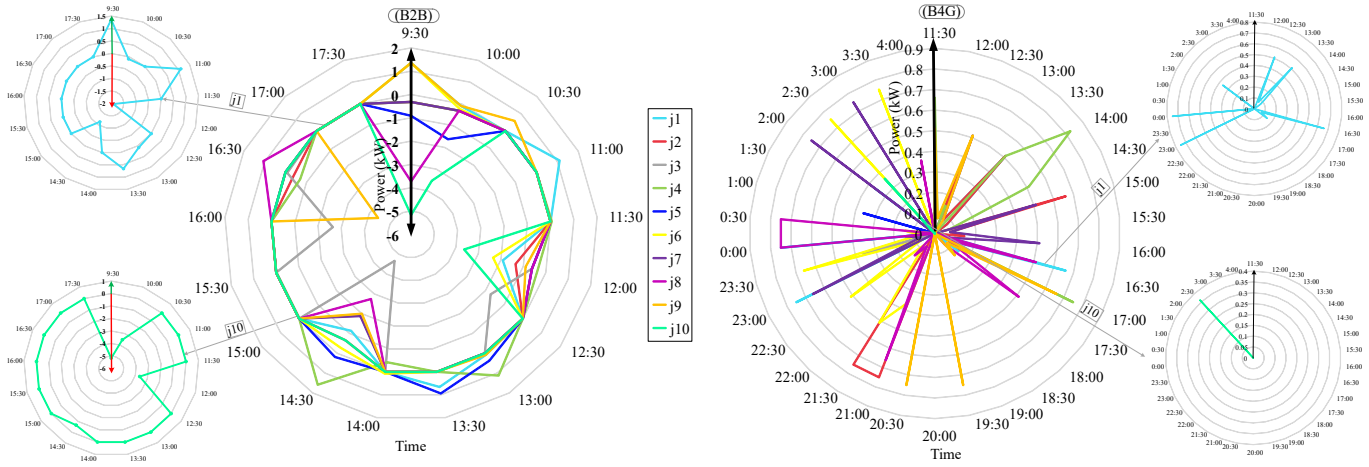

Fig. 8: Power exchange in B2B and B4G strategies.

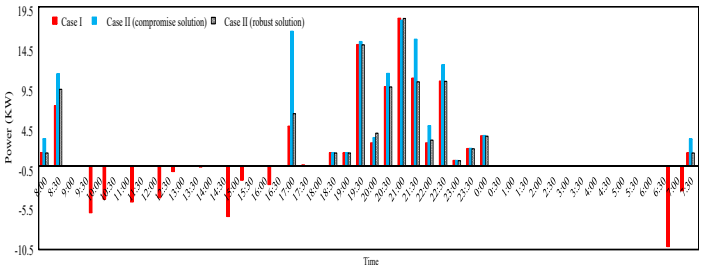

Fig. 9: Energy exchange with the main grid in different cases.

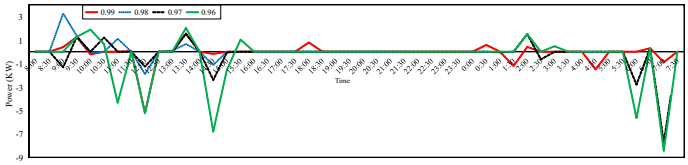

Fig. 10: Variation of B2B value over different levels of occupants comfort.

behaviour, while B4G strategy can be efficient for ABs with a higher operational profile.

D. Energy Exchange with the Main Grid

The energy exchange between RMG and the main grid in cases I and II is shown in Fig. 9. This figure shows that utilising the B2B and B4G strategies affected the power exchange with the main grid. The energy export to the main grid is zero in Case II (both scenarios). This demonstrates that ABs with excess generation have sold their power to other buildings, while those with energy needs purchased energy locally rather than importing from the main grid (see Fig. 8). This strategy can be an effective alternative for profit-seeking retailers who try to achieve a high retail profit from prosumers by offering high sell prices and low buy prices. In the grid level, it can delay the need for generation investment. On the other hand, comparing robust and compromise solutions of Case II shows how more grid power import occurs in former compared to latter. For example, at 17:00, the imported power from the main grid in robust solution is almost twice as much as that of compromise solution. This means that the decision made by RRH controller is robust against higher price deviation. In other words, in order to improve the robustness against the higher price deviation, the imported power is decreased or at least not changed, especially during high market price periods (i.e. from 19:30 to 23:00).

E. Role of Occupants

The effect of occupants comfort on the B2B interaction is illustrated in Fig. 10, where the power exchange of building j_1 over the control horizon is depicted for different levels of occupants comfort. As can be seen in this figure, building exchanged more power in the local market at lower values of occupants comfort index (i.e. 0.96). However, increasing the value of occupants comfort index resulted in a considerable decrease in participation of building in the local market. Therefore, social factors (i.e. occupant behaviour) can have a considerable influence on the energy interaction in the local markets.

The participation of occupants in improving the system robustness should not be neglected. Fig. 11 highlights the contribution of occupants in improving system robustness, by giving an example of the indoor temperature in robust and compromise scenarios of Case II for building j_1. In the compromise solution, the main goal of controller is to keep the temperature around the preferred set point given by the AB while considering the economic factors. Robust solution, however, experiences more fluctuation and lower temperatures, particularly under high market price periods (i.e. from 19:30 to 23:00). This demonstrates that AB occupants can have a considerable role in improving the RMG robustness by alternating their preferred comfort zones. These variations in the temperature of building has affected the comfort index, as shown in Fig. 11. It is evident from this figure that the comfort index of the AB fluctuated over the price variations, with slightly lower values in the robust solution. The result obtained for robust solution also shows that how ABs can allow the controller to oversee a flexible indoor temperature in response to market price. In doing so, the building thermal inertia is utilised as an energy storage mechanism and indoor temperature is increased to above the set point in morning hours with lower market price and thereafter allowed to fall gradually. The intrinsically slow thermal response of most buildings is a major advantage to exploit as a virtual thermal storage resources. Thermal neutrality (or the ability of an AB to stay within comfort bands) is even more pronounced in well-insulated buildings.

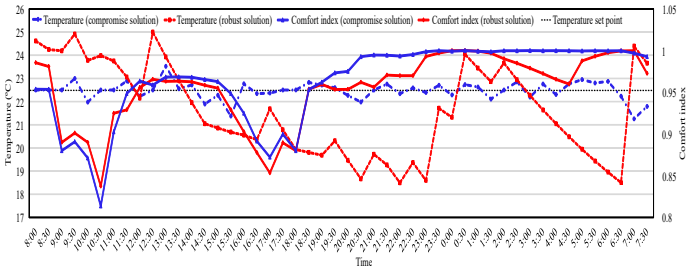

Fig. 11: Variation of temperature and comfort index of building j_1 over the operation horizon for different cases.

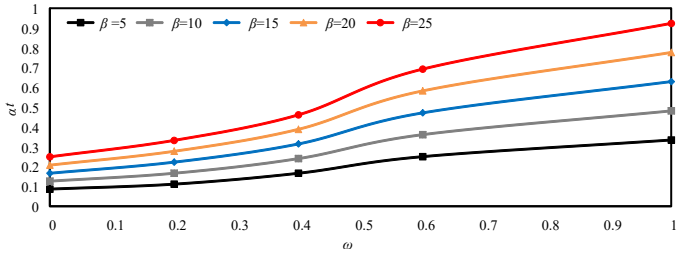

Fig. 12: Variation of robustness over ω for different value of β.

F. Robustness Analysis

In the proposed RRH model, the tolerable value of robustness (i.e. β) and the robustness degrees' weighting factor (i.e. ω) are instrumental in how the robustness degree component performs. This is demonstrated by a sensitivity analysis in Fig. 12 that examines variation of α^t over the weighting factor ω for various levels of β. This figure shows that increasing ω raises the value of α^t. This can be interpreted with Equation (34) in mind, that increasing ω raises the weight of weather-related robustness, resulting in a dramatic increase in the value of α^t. In another words, it is easier to increase the weather-related robustness as opposed to that of the market price. Besides, increasing the value of β raises the robustness degree.

G. Computational Efficiency

In order to evaluate the computational and economic merits of the proposed model, it is benchmarked against the conventional rolling horizon method within three different scenarios: [I] S_1 which portrays an optimistic future horizon in which predicted data and the subsequent reality for those forecasts are the same; [II] S_2 with across a 3 hour future horizon assumes the real weather to be 30% different to the initial forecast and the market price to be 15% different to the initial value and finally [III] S_3 which solves the same optimisation problem as S_1 using 5-min intervals (instead of 30 min). The results for these scenarios are outlined against the proposed RRH in Table III. Scenario S1 solves the model in 34.21s at each time step, while the proposed RRH model takes 42.15s. Comparing scenarios S_1 and S_2 shows that deviations between initial forecast and subsequent reality results in more operational cost. To overcome this problem, S_3 solved the model at finer time intervals that yields 8.6% cost reduction (compared to S_2), but at a penalty of much higher computational time (i.e. 175.25 seconds each iteration). Against these results, the proposed RRH demonstrated superior performance in both computational (e.g. 76% lower compared to S_3) and economic aspects (e.g. 6.3% lower cost as opposed to S_2). The improved accuracy in scenario S_3 imposes considerably higher processing and computational costs which may be viewed as excessive in a residential context. These factors highlights the potential of the proposed RRH as an effective option for controlling RMGs.

TABLE III: Computation efficiency of different techniques.

Scenario (time step)	Computation time (Sec.) Per interval	Total	Operational cost (£)	Comfort index
S_1 (30 min.)	34.21	1,648.08	6.35	0.986
S_2 (30 min.)	34.21	1,648.08	7.13	0.985
S_3 (5 min.)	175.25	50,472.00	6.51	0.976
RRH (30 min.)	41.15	2,023.20	6.68	0.973

TABLE IV: Comparison of MILP and MINLP models.

Model type	MINLP		MILP	
Solver	BARON	DICOPT	CPLEX	MOSEK
Computation time (min. per interval)	54.05	9.67	0.70	1.92
Operational cost(£)	6.70	6.70	6.68	6.68
Comfort index	0.973	0.973	0.973	0.973
Relative gap (%)	0	0	0	0

Finally, the computational time and accuracy of the proposed RRH controller, derived from the proposed MILP model is compared with those of MINLP model in Table IV, using different solvers. As shown in this table, the relative gap of zero is considered for the model, demonstrating the optimality of the solution obtained from the MILP model. This index shows the difference between the best integer and the best estimate solutions. As described in [36], zero or small relative gap is the indicator of measure of optimality and accuracy of the optimisation model. Furthermore, comparing the MILP and MINLP model demonstrates that the main issue for the later is its computational time. The BARON solver demanded 54.05 minutes for each time interval (i.e. 30 minutes), while DICOPT solved the model in 9.67 minutes. High computational time could be a barrier for MINLP models in a real-time application; since as per our finding, the computational time of BARON solver is twice the duration of the simulation time interval. The MILP solvers achieved a considerably lower computation time while also delivering the same comfort index (Table IV). A marginal difference is observed in the operational cost of MINLP and MILP models, which does not question the accuracy of Equation (42), and the whole formulation. Considering the residential skill of the proposed framework, it is important to achieve acceptable results without demanding an expensive processor. Besides, such control framework should be fast enough when considering the dynamics of the grid [21]. To summarise, these results show that the solutions of MILP model reflect those of original model, while achieving a significantly lower computational time.

VII. Conclusions

In this study, a multi-objective multi-level optimisation model is proposed for control and scheduling of RMGs, consisting of a community of buildings and several small-scale distributed energy resources. An RRH controller is introduced which boosts the robustness of the system operation in the face of constant and uncertain changes over a short-term horizon. With an MILP model, the proposed controller benefits from considerably lower computation time when benchmarked against conventional methods. The role of ABs in energy networks is highlighted by introducing B2B and B4G strategies. The importance of social factors in the energy exchange between buildings is investigated through analysing the effect of occupants comfort on the building flexibility measures.

Also, the role of building occupants in improving the system robustness in face of uncertain input data is analysed. The simulation results indicate human comfort and energy cost savings of these strategies and the efficiency of the RRH controller. Notable findings of this study are:

- The B2B and B4G strategies are a viable approaches which exploit differences in timing and extent of occupant thermo-visual comfort to deliver an optimal comfort solution at community level while providing techno-economic advantages for the main grid.
- Utilising the B2B and B4G strategies in a local market level can create potential energy transaction between dwellings, which can bring about cost saving for the community. This can also delay the generation investment in a higher level.
- The RMG controller can be an efficient solution for the conventional thermostats. This controller can achieve desirable comfort zones while decreasing the energy bill.
- If the controller has the autonomy to decrease comfort expectation of AB occupants by 1.3%, the control robustness is improved by 10%. This shows the considerable role of building occupants in improving system robustness in face of uncertainty.
- Building occupants can play a critical role in energy exchange between dwelling. Increasing the occupants expectation in terms of comfort level can have a direct influence on the building participation in the local market.
- The RRH approach reduced the total computation time by approximately 76% when compared with the conventional controllers that for similar comfort and cost optimisation need to shorten simulation intervals from 30min to 5min leading to high computational penalties.

Future research studies can examine the role of B2B strategies in the energy network. The interconnection between different communities could bring about more advantages for the network and users. The integration of issues arising from public health measures in the operation of RMGs can be another research direction which can study the effect of pandemic issues on the behaviour of buildings and the way they can contribute in emergency conditions.

ACKNOWLEDGMENT

This work was made possible through funding from Newcastle University and Engineering and Physical Sciences Research Council grant EP/S016627/1: Active building Centre. The authors would like to thanks Mr. Malcolm Hill for his valuable comments regarding the preparation of the manuscript.

REFERENCES

[1] A. building center, "How can active buildings reduce uk carbon emission?" https://www.activebuildingcentre.com, 2019.

[2] Kroposki, Benjamin and Bernstein, Andrey and King, Jennifer and Ding, Fei . (November 2020) Tomorrow's Power Grid Will Be Autonomous. [Online]. Available: https://spectrum.ieee.org/energy/the-smarter-grid/tomorrows-power-grid-will-be-autonomous

[3] T. Sousa, T. Soares, P. Pinson, F. Moret, T. Baroche, and E. Sorin, "Peer-to-peer and community-based markets: A comprehensive review," *Renewable and Sustainable Energy Reviews*, vol. 104, pp. 367–378, 2019.

[4] J. Bialek, "What does the GB power outage on 9 August 2019 tell us about the current state of decarbonised power systems?" *Energy Policy*, vol. 146, p. 111821, 2020.

[5] A. F. Crossland, D. Jones, N. S. Wade, and S. L. Walker, "Comparison of the location and rating of energy storage for renewables integration in residential low voltage networks with overvoltage constraints," *Energies*, vol. 11, no. 8, p. 2041, 2018.

[6] D. Zhang, S. Liu, and L. G. Papageorgiou, "Fair cost distribution among smart homes with microgrid," *Energy Conversion and Management*, vol. 80, pp. 498–508, 2014.

[7] F. Luo, W. Kong, G. Ranzi, and Z. Y. Dong, "Optimal home energy management system with demand charge tariff and appliance operational dependencies," *IEEE Transactions on Smart Grid*, vol. 11, no. 1, pp. 4–14, 2019.

[8] S. Khanna, V. Becerra, A. Allahham, D. Giaouris, J. M. Foster, K. Roberts, D. Hutchinson, and J. Fawcett, "Demand response model development for smart households using time of use tariffs and optimal control—the isle of wight energy autonomous community case study," *Energies*, vol. 13, no. 3, p. 541, 2020.

[9] C. Keles, A. Karabiber, M. Akcin, A. Kaygusuz, B. B. Alagoz, and O. Gul, "A smart building power management concept: Smart socket applications with dc distribution," *International Journal of Electrical Power & Energy Systems*, vol. 64, pp. 679–688, 2015.

[10] O. Van Cutsem, D. H. Dac, P. Boudou, and M. Kayal, "Cooperative energy management of a community of smart-buildings: A blockchain approach," *International Journal of Electrical Power & Energy Systems*, vol. 117, p. 105643, 2020.

[11] Y. Huang, L. Wang, W. Guo, Q. Kang, and Q. Wu, "Chance constrained optimization in a home energy management system," *IEEE Transactions on Smart Grid*, vol. 9, no. 1, pp. 252–260, 2016.

[12] M. Royapoor, M. Pazhoohesh, P. J. Davison, C. Patsios, and S. Walker, "Building as a virtual power plant, magnitude and persistence of deferrable loads and human comfort implications," *Energy and Buildings*, p. 109794, 2020.

[13] L. Hurtado, P. Nguyen, and W. Kling, "Smart grid and smart building inter-operation using agent-based particle swarm optimization," *Sustainable Energy, Grids and Networks*, vol. 2, pp. 32–40, 2015.

[14] F. Wang, L. Zhou, H. Ren, X. Liu, S. Talari, M. Shafie-khah, and J. P. Catalao, "Multi-objective optimization model of source–load–storage synergetic dispatch for a building energy management system based on tou price demand response," *IEEE Transactions on Industry Applications*, vol. 54, no. 2, pp. 1017–1028, 2017.

[15] H. O. Alwan, H. Sadeghian, and S. Abdelwahed, "Energy management optimization and voltage evaluation for residential and commercial areas," *Energies*, vol. 12, no. 9, p. 1811, 2019.

[16] A. Ahmad and J. Y. Khan, "Real-time load scheduling, energy storage control and comfort management for grid-connected solar integrated smart buildings," *Applied Energy*, vol. 259, p. 114208, 2020.

[17] G. S. Georgiou, P. Christodoulides, and S. A. Kalogirou, "Real-time energy convex optimization, via electrical storage, in buildings–a review," *Renewable energy*, 2019.

[18] R. AhmadiAhangar, A. Rosin, A. N. Niaki, I. Palu, and T. Korõtko, "A review on real-time simulation and analysis methods of microgrids," *International Transactions on Electrical Energy Systems*, vol. 29, no. 11, p. e12106, 2019.

[19] J. A. Pinzon, P. P. Vergara, L. C. Da Silva, and M. J. Rider, "Optimal management of energy consumption and comfort for smart buildings operating in a microgrid," *IEEE Transactions on Smart Grid*, vol. 10, no. 3, pp. 3236–3247, 2018.

[20] D. Wu, H. Zeng, C. Lu, and B. Boulet, "Two-stage energy management for office buildings with workplace ev charging and renewable energy," *IEEE Transactions on Transportation Electrification*, vol. 3, no. 1, pp. 225–237, 2017.

[21] M. Razmara, G. R. Bharati, M. Shahbakhti, S. Paudyal, and R. D. Robinett, "Bilevel optimization framework for smart building-to-grid systems," *IEEE transactions on Smart Grid*, vol. 9, no. 2, pp. 582–593, 2016.

[22] C. A. Correa-Florez, A. Gerossier, A. Michiorri, and G. Kariniotakis, "Stochastic operation of home energy management systems including battery cycling," *Applied energy*, vol. 225, pp. 1205–1218, 2018.

[23] A. Akbari-Dibavar, S. Nojavan, B. Mohammadi-Ivatloo, and K. Zare, "Smart home energy management using hybrid robust-stochastic optimization," *Computers & Industrial Engineering*, p. 106425, 2020.

[24] A. Najafi-Ghalelou, S. Nojavan, and K. Zare, "Heating and power hub models for robust performance of smart building using information gap decision theory," *International Journal of Electrical Power & Energy Systems*, vol. 98, pp. 23–35, 2018.

[25] M. Ban, M. Shahidehpour, J. Yu, and Z. Li, "A cyber-physical energy management system for optimal sizing and operation of networked nanogrids with battery swapping stations," *IEEE Transactions on Sustainable Energy*, vol. 10, no. 1, pp. 491–502, 2017.

[26] A. Soroudi and T. Amraee, "Decision making under uncertainty in energy systems: State of the art," *Renewable and Sustainable Energy Reviews*, vol. 28, pp. 376–384, 2013.

[27] U. R. Nair and R. Costa-Castelló, "A model predictive control-based energy management scheme for hybrid storage system in islanded microgrids," *IEEE access*, vol. 8, pp. 97 809–97 822, 2020.

[28] T. Morstyn, N. Farrell, S. J. Darby, and M. D. McCulloch, "Using peer-to-peer energy-trading platforms to incentivize prosumers to form federated power plants," *Nature Energy*, vol. 3, no. 2, pp. 94–101, 2018.

[29] C. Long, J. Wu, C. Zhang, L. Thomas, M. Cheng, and N. Jenkins, "Peer-to-peer energy trading in a community microgrid," in *2017 IEEE power & energy society general meeting*. IEEE, 2017, pp. 1–5.
[30] M.-A. Nasr, S. Nikkhah, G. B. Gharehpetian, E. Nasr-Azadani, and S. H. Hosseinian, "A multi-objective voltage stability constrained energy management system for isolated microgrids," *International Journal of Electrical Power & Energy Systems*, vol. 117, p. 105646, 2020.
[31] A. Soroudi, A. Rabiee, and A. Keane, "Information gap decision theory approach to deal with wind power uncertainty in unit commitment," *Electric Power Systems Research*, vol. 145, pp. 137–148, 2017.
[32] Y. Ben-Haim, *Info-gap decision theory: decisions under severe uncertainty*. Elsevier, 2006.
[33] A. Soroudi, *Power system optimization modeling in GAMS*. Springer, 2017, vol. 78.
[34] Nikkhah, Saman and Giaouris, Damian and Bialek, Janusz and Allahham, Adib and Royapoor Mohammad . (December 2020) Active Building Data. [Online]. Available: https://data.ncl.ac.uk/articles/dataset/Energy_scheduling/13387280/1
[35] J. Rouleau and L. Gosselin, "Impacts of the covid-19 lockdown on energy consumption in a canadian social housing building," *Applied Energy*, vol. 287, p. 116565, 2021.
[36] K. Chen, W. Wu, B. Zhang, S. Djokic, and G. P. Harrison, "A method to evaluate total supply capability of distribution systems considering network reconfiguration and daily load curves," *IEEE Transactions on Power systems*, vol. 31, no. 3, pp. 2096–2104, 2015.

Saman Nikkhah (GSM'20) received the B.Sc. degree from the Urmia University, Urmia, Iran in 2013, and the M.Sc. (Hons.) degree from the University of Zanjan, Zanjan, Iran, in 2016. He is currently a Ph.D. student in the School of Engineering, Newcastle University, Newcastle upon Tyne, UK. His research interests include active buildings, integrated energy systems, smart grid, resilience, and voltage stability.

Adib Allahham received the B.S. degree in Electric Engineering from Damascus University, Syria, and the M.Sc. and Ph.D. degrees from the Joseph Fourier University of Grenoble, France, in 2004 and 2008, respectively. From 1999 to 2003, he worked at the energy industry. In 2008, he joined the G-SCOP Laboratory, France, as a Postdoctoral Researcher. From 2009 to June 2016, he worked as a Senior Lecturer with the Electrical Power Engineering Department, Damascus University. Since 2016, he has been a Researcher with the School of Engineering, Newcastle University. He has published more than 30 peer-reviewed journal and international conference papers. His research interests include the energy storage systems, smart grid technologies, grid connected renewable energy sources, and multi-vector energy integration.

Mohammad Royapoor received B.Eng. and M.Eng. degrees in Building Services Engineering from Northumbria University in 2009 and 2010, respectively, and PhD in building climate control using adaptive comfort in 2014. Since 2013 he has held post-doctoral research roles at Sir Joseph Swan Centre for Energy Research and National Centre for Energy Systems Integration (Newcastle University). His research roles had included examination of novel tri-generation systems, off-grid zero carbon power, heating and cooling solutions for developing countries, quantification of building demand response capabilities and design and control of smart local energy systems.

Janusz Bialek (F'11) received his M.Eng. and Ph.D. degrees in Electrical Engineering from Warsaw University of Technology, Poland. Currently, he is Professor of Power and Energy Systems at Newcastle University, UK, and Full Professor at Skolkovo Institute of Science and Technology (Skoltech), Russia, where he was the founding Director of Center for Energy Systems. Previously he held Full Professor positions at the University of Edinburgh (2003-2009) and Durham University (2009-2014). His main research interests are in the application of advanced mathematical methods to address techno-economic problems of achieving low-carbon power systems and preventing blackouts.

Damian Giaouris received the B.Eng. degree in automation engineering from the Technological Educational Institute of Thessaloniki, Thessaloniki, Greece, in 2000, the B.Sc. degree and Postgraduate Certificate in Mathematics from Open University, Milton Keynes, UK, in 2009 and 2011, respectively, and the M.Sc. and Ph.D. degrees in the area of control of electrical systems from Newcastle University, Newcastle upon Tyne, UK, in 2001 and 2004, respectively. He was a Lecturer in Control Systems with Newcastle University, since 2004, before moving to the Centre for Research and Technology Hellas (Greece), in 2011. Since September 2015, he has been a Senior Lecturer in Control of Electrical Systems and a Reader of Control of Energy Systems with Newcastle University. His research interests include control of power converters, power systems, smart grids, electric vehicles, and nonlinear dynamics of electrical systems. He has been in various editorial boards and has more than 150 publications.